



## Classification of the frozen/thawed surface state of Northern land areas based on SMAP and GCOM-W1 brightness temperature observations at 1.4 GHz and 6.9 GHz

Konstantin Muzalevskiy, Zdenek Ruzicka, Alexandre Roy, Michael M. Loranty & Alexander Vasiliev

To cite this article: Konstantin Muzalevskiy, Zdenek Ruzicka, Alexandre Roy, Michael M. Loranty & Alexander Vasiliev (2021) Classification of the frozen/thawed surface state of Northern land areas based on SMAP and GCOM-W1 brightness temperature observations at 1.4 GHz and 6.9 GHz, Remote Sensing Letters, 12:11, 1073-1081, DOI: [10.1080/2150704X.2021.1963497](https://doi.org/10.1080/2150704X.2021.1963497)

To link to this article: <https://doi.org/10.1080/2150704X.2021.1963497>



Published online: 15 Sep 2021.



Submit your article to this journal [↗](#)



Article views: 41



View related articles [↗](#)



View Crossmark data [↗](#)



# Classification of the frozen/thawed surface state of Northern land areas based on SMAP and GCOM-W1 brightness temperature observations at 1.4 GHz and 6.9 GHz

Konstantin Muzalevskiy<sup>a</sup>, Zdenek Ruzicka<sup>a</sup>, Alexandre Roy<sup>b</sup>, Michael M. Loranty<sup>c</sup> and Alexander Vasiliev<sup>d</sup>

<sup>a</sup>Laboratory of Radiophysics of the Earth Remote Sensing, Kirensky Institute of Physics Federal Research Center KSC Siberian Branch Russian Academy of Sciences (Iph SB RAS), Krasnoyarsk, Russia; <sup>b</sup>Université du Québec à Trois-Rivières (UQTR), Département des Sciences de l'Environnement, Trois-Rivières, Canada, Centre d'étude Nordique, Québec, Canada; <sup>c</sup>Department of Geography, Colgate University, Hamilton, NY, USA; <sup>d</sup>Earth Cryosphere Institute, Tyumen Scientific Centre SB RAS, Russian Federation, Tyumen

## ABSTRACT

In this letter, the method created earlier by the authors and the information product *SPL3FTP\_E* of the Soil Moisture Active Passive (SMAP) satellite for determining frozen/thawed state of soil surface on the example of test sites placed on North Slope of Alaska, U.S.A., Canada, Finland and Russian Federation were compared. As an indicator of the frozen/thawed state of soil surface, the polarization index calculated on the basis of the reflectivity of soils was proposed. The soil reflectivity was determined in the L-band based on the SMAP radiometric observations at a frequency of 1.4 GHz using the values of brightness temperatures measured by the Global Change Observation Mission – Water 1/Advanced Microwave Scanning Radiometer 2 (GCOM-W1/AMSR2) at a vertical polarization and a frequency of 6.9 GHz, as an estimate of the soil effective temperature. As a result, it was shown that the developed method makes it possible to increase accuracy of the frozen/thawed states determination of soil surface from 3% to 9% in relation to the SMAP data (*SPL3FTP\_E*) for twelve Arctic test sites.

## ARTICLE HISTORY

Received 19 March 2021  
Accepted 27 July 2021

## 1. Introduction

Recently, there has been development of algorithms of land surface frozen/thawed (FT) state that employ radiometric observations at L-band from the Aquarius (Roy et al. 2015), Soil Moisture and Ocean Salinity (SMOS) (Rautiainen et al. 2016, 2014; Roy et al. 2015) and Soil Moisture Active Passive (SMAP) (Derksen et al. 2017; Dunbar et al. 2016) satellites. These FT algorithms are based on a seasonal threshold approach that examines the time series progression of the normalized polarization ratio (NPR), calculated from radiometer measurements, relative to signatures acquired during seasonal reference frozen and thawed states (Rautiainen et al. 2014). Another approach using higher frequency estimates of quasi-temperature and quasi-emissivity have been used to classify FT state (Zhao

**CONTACT** Konstantin Muzalevskiy  [rsdkm@ksc.krasn.ru](mailto:rsdkm@ksc.krasn.ru)  Laboratory of Radiophysics of the Earth Remote Sensing, Kirensky Institute of Physics Federal Research Center KSC Siberian Branch Russian Academy of Sciences (Iph SB RAS), Krasnoyarsk, Russia

et al. 2011, 2017; Hu et al. 2017, 2019), based on Advanced Microwave Scanning Radiometer for EOS (AMSR-E) polarimetric measurements of brightness temperatures at frequency of 18.7 GHz and 36.5 GHz. The main idea proposed in these research (Zhao et al. 2011, 2017; Hu et al. 2017, 2019) was to project a two-dimensional time series array (quasi-temperature and quasi-emissivity) into a one-dimensional space of a discriminant function using the Fisher approach (Fisher 1936). Then, regression analysis was used to establish a correlation between the discriminant function and soil temperature in the upper 5 cm. Muzalevskiy and Ruzicka (2020) showed that the polarization ratio index, calculated from reflectivity values, rather than the polarization ratio index calculated using brightness temperatures values, significantly improved the possibility of determining the reference values of frozen and thawed soil states. The novelty of the proposed approach lies in the method for estimating reflectivity of soil from SMAP radiometric data using the values of V-polarized brightness temperature measured by the Advanced Microwave Scanning Radiometer 2 (AMSR2) radiometer at 6.9 GHz to characterize the effective temperature of the topsoil. Taking into account that the Copernicus Imaging Microwave Radiometer (Kilic et al. 2018) is expected to be launched in 2028, equipped with a high spatial resolution multispectral radiometer 1.4–36.5 GHz (55–5 km), the development of multifrequency algorithms for classifying the FT state of land surface is relevant. In this letter, the results of further validation of the new method (Muzalevskiy and Ruzicka 2020), with respect to the SMAP freeze/thaw product over an expanded number of test sites, equipped with soil-climatic weather stations, located in geographically different Northern land areas are presented.

## 2. Test sites, in situ and satellites data

### 2.1. Test sites and in-situ data

To validate the new method (Muzalevskiy and Ruzicka 2020), 12 test sites were selected. These sites are located in different parts of the northern regions (see Figure 1): the North Slope of Alaska, U.S.A., North Canada, Finland and Russia and are equipped with soil-climatic meteorological stations. The coordinates of test sites, land cover type and period of observations are given in Table 1. In Table 1, land cover characteristics (ESA 2017) are calculated for a rectangle 40 km × 40 km with a centre corresponding to weather station coordinate. Test sites are represented by a variety of tundra landscapes with spars vegetation, lichens/mosses, grassland, shrubs Deadhorse (DH), Franklin Bluffs (FB), Sagwon (SG), Happy Valley (HV), Imnaviat

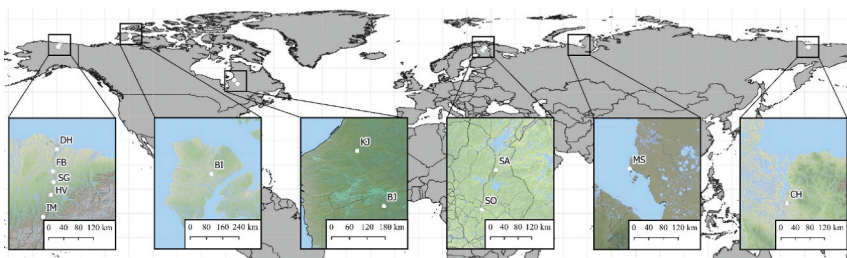


Figure 1. Location map of test sites.

**Table 1.** Characteristics of test sites and periods of observation.

Test sites	Location	Longitude/ Latitude	Percentage of land cover types (%)	Bioclimaticsubzone (Walker et al. 2005)	Period of observation
Deadhorse (DH)	Alaska, U.S.A.	−148.4653°W/ 70.1613°N	e: 61, g: 19, c: 12, f: 8	C–D (coastal plain)	1 April 2015– 30 June 2019
Franklin Bluffs (FB)	Alaska, U.S.A.	148.7208°W/ 69.6741°N	e: 81, b: 6, g: 6, f: 4, d: 2	D (coastal plain)	24 August 2016– 29 March 2019
SagMAT/ MNT (SG)	Alaska, U.S.A.	148.6739°W/ 69.4330°N	e: 71, b: 20, g: 3, f: 3, d: 3	E (gentle hills)	1 April 2015– 22 August 2018
Happy Valley (HV)	Alaska, U.S.A.	148.8483°W/ 69.1466°N	e: 57, b: 38, d: 2, g: 1, f: 1	E (hills)	1 April 2015– 1 March 2019
Imnaviat (IM)	Alaska, U.S.A.	149.3523°W/ 68.6397°N	e: 78, b: 16, f: 2, d: 2, g: 2	E (hills)	1 April 2015– 30 June 2019
Banks Island (BI)	Inuvik, Canada	119.5615°W/ 73.2200°N	e: 97, g: 3	C (coastal plain)	1 April 2015– 30 June 2019
Baie-James (BJ)	Quebec, Canada	75.0134°W/ 53.4070°N	a: 67, d: 16, g: 12, b: 2, e: 2	Borealforest	1 April 2015– 30 June 2019
Lake Chisapaw (KJ)	Quebec, Canada	76.3141°W/ 54.9731°N	a: 60, d: 20, g: 10, e: 9	Borealforest	30 August 2016– 19 May 2019
Sodankylä (SO)	Finland	26.6333°E/ 67.3621°N	a: 85, c: 12, g: 3	Borealforest	1 April 2015– 31 May 2019
Saariselka (SA)	Finland	27.5506°E/ 68.3302°N	a: 70, c: 23, e: 5, b: 1	Borealforest	1 April 2015– 31 May 2019
Maresale (MS)	Yamal, Russia	66.8100°E/ 69.7100°N	e: 69, g: 11, b: 12, d: 5, a: 3	D (coastal plain)	18 August 2015– 18 May 2019
Cherski (CH)	Yakutia, Russia	161.4819°E/ 68.7475°N	a: 53, c: 20, g: 19, f: 5	E (coastal plain)	1 April 2015– 31 March 2018

a – Forest; b – Grassland; c – Wetland; d – Shrubland; e – Sparse vegetation; f – Bare area; g – Water.

(IM), Maresale (MS) and boreal forests Baie-James (BJ), Lake Chisapaw (KJ), Saariselka (SA), Sodankylä (SO). At DH and Cherski (CH) are more of water bodies (19.4%, 18.8%) and wetland areas (11.9%, 20.4%). More than 10% of the pixels consist of water bodies at MS (10.9%), KJ (10.3%) and BJ (12.4%). At the North Slope of Alaska, test sites soil temperature was measured at a surface (depth of 1 cm). DH and FB test sites located in coastal plain with flat alluvial terrace. Moss tundra landscape of the test sites dominantly formed moist non-acidic sedges, prostrate-shrubs. SG, HV and IM located on hilly terrain with dominantly moist acidic and non-acidic tussock tundra to the north and considerable shrub growth to the south. Boreal forest test sites are represented by SO, SA in Finland and BJ, KJ in Canada. SO and SA are located in different density forest, non-forest area is covered with juniper, heather and thin layer of lichen and moss. BJ and KJ are located in typical Canadian taiga with low-density black spruce-lichen woodland (sandy soils). Soil temperature at the test sites were measured at a depth of 2–5 cm. On Yamal peninsula MS (5 km from the coastline of the Kara Sea) test site was chosen. Test sites located in moist and dry dwarf shrub-moss-lichen tundra in combination with sedge-moss mires. The soil temperature on MS was measured at a depth of 2–5 cm. At CH test site soil temperature was measured in five test plots (which averaged for further analysis) at the interface between the organic and mineral soil layers, at depths of 6–10 cm below the surface depending on organic layer thickness. All plots are within larch forests with different density of trees, where percent canopy cover ranges from 13% to 75%.

## 2.2. SMAP, GCOM-W1(AMSR2) brightness temperature and auxiliary MODIS LST data

At a frequency of 1.41 GHz, SMAP polarimetric brightness temperature data (SPL3FTP\_E) in Northern Hemisphere azimuthal projections on a 9 km Equal-Area Scalable Earth Grid (EASE-Grid 2.0) were used over the test sites in the period of soil temperature observations by the weather stations (see Table 1). Brightness temperature data at a frequency of 6.925 GHz were acquired from the AMSR2 on-board Global Change Observation Mission – Water 1 (GCOM-W1) satellite, gridded with 12.5 km resolution. SMAP and AMSR2 brightness temperature observations were used both for ascending and descending orbits. The difference in observation angles 40° and 55°, respectively for SMAP and AMSR2, was neglected. Pixels closest to the coordinates of weather stations, with the exception of MS, were used in the analysis. MS is located at the coast of the Kara Sea, thus a pixel whose centre is far more than 50 km from the sea was chosen. Daily 9 km EASE-Grid freeze/thaw SMAP product (SPL3FTP\_E, both ascending and descending orbits) based on the NPR index (Dunbar et al. 2016) was used for identification freeze/thaw state of land at the test sites. From the Moderate Resolution Imaging Spectroradiometer (MODIS) Land Surface Temperature (LST) of the MYD11A1 data product was used. MYD11A1 is a daily product and provides day and night LST. LST was used to additionally check unexpected (respect to SMAP SPL3FTP\_E product) freeze/thaw events in the North Slope of Alaska.

## 3. The method of freeze/thaw soil state determination

As the FT state indicator of soil surface, it was proposed to use the polarization index  $MPR = \frac{1}{2} \frac{\Gamma_H + \Gamma_V}{\Gamma_H - \Gamma_V}$ , for the calculation of which reflectivity estimated at the horizontal  $\Gamma_H$  and vertical  $\Gamma_V$  polarizations were used. This is in contrast to works (Derksen et al. 2017; Dunbar et al. 2016; Rautiainen et al. 2016), in which the values of brightness temperatures  $T_{BH}$  and  $T_{BV}$  on horizontal and vertical polarizations are used to calculate the polarization index  $NPR = \frac{1}{2} \frac{T_{BV} - T_{BH}}{T_{BV} + T_{BH}}$ . Reflectivity in the L-band  $\Gamma_{H,V} = 1 - \frac{T_{BH,V}}{T_{BV6.9}}$  was determined based on SMAP radiometer brightness temperature  $T_{BH,V}$  and GCOM-W1/AMSR2 radiometer brightness temperature, measured at vertical polarization and a frequency of 6.9 GHz as the estimation of effective soil surface temperature (Muzalevskiy and Ruzicka 2020; Muzalevskiy et al. 2016). For test sites placed in the North Slope of Alaska and Russia, a significant correlation between the transitions of MPR index through a certain threshold level and the transitions of soil surface temperature through 0°C was demonstrated (Muzalevskiy and Ruzicka 2020). To quantitatively compare the results of FT state between SMAP product (Dunbar et al. 2016) and assessment based on the proposed MPR index, a normalized index nMPR was calculated using the formula  $nMPR = \frac{MPR(t) - MPR_{fr}}{MPR_{th} - MPR_{fr}}$ , where  $MPR(t)$  is the current value of the index,  $MPR_{fr}$  and  $MPR_{th}$  is the average value of the index for the frozen and thawed soil. Threshold levels of  $MPR = 1.0$  and  $nMPR = 0.75$  for both ascending and descending orbits were chosen to identify the soil's FT state. On average, these levels corresponded to the transition of soil surface temperature through 0°C (based on the weather stations data from 2015 to 2019). The soil was considered stable-frozen or thawed if the temperature of soil surface according to the data of meteorological stations was more or less 0°C for more than 14 days, respectively.

## 4. Results and discussion

The FT states are determined on 11.1/14.9 days earlier and on 18.9/19.3 days later in the case of thawed and frozen soil, respectively, based on the nMPR/MPR indices (ascending orbits) relative to the weather stations data (see Figure 2(a and b)). For descending orbits, the FT states are determined on 11.4/11.3 days earlier and on 18.3/19.9 days later in the case of thawed and frozen soil, respectively, based on the nMPR/MPR indices relative to the weather stations data. (These estimates are given in terms of root mean square error (RMSE)). Relative to the weather station data, determination of FT state based on the SPL3FTP\_E data takes place on 22.0/24.0 days earlier and on 19.8/18.4 days later, respectively, for the ascending/descending orbits of SMAP (see Figure 2(c)). The number of days (as a percentage of the total number of days on which satellite observations were made) for which the soil FT state was identical identified both based on satellite observations (using the MPR, nMPR and SPL3FTP\_E product) and meteorological stations data (surface soil temperature) are given in Table 2 for the period from April 2015 to June 2019. Thus defined, this percentage of satellite observation days will be referred as accuracy in the determination of soil FT state. The use of nMPR and MPR indices allows (see Table 2) increases the reliability of FT state determination in relation to the standard SMAP algorithm (SPL3FTP\_E) on average by 8–9% and 3–7%, respectively for ascending and descending orbits. In the case of ascending orbits, RMSE/coefficient of determination ( $R^2$ ) between the days of the year (DOY) for which FT state had been determined based on indexes of MPR, nMPR, and SMAP SPL3FTP\_E product and the weather stations data is 19.7 days/0.95, 18.9 days/0.96, and 27.1 days/0.91, respectively (see Figure 2). For descending orbits similar estimates of RMSE/ $R^2$  appeared to be equal of 30.4 days/0.89 in case of SPL3FTP\_E product and do not practically change in case of MPR, and nMPR indexes. nMPR index performs slightly better accuracy than the MPR index (see Table 2 and Figure 2) due to normalization MPR index by the reference MPR values corresponding to the frozen and thawed states of soil. In additional analysis, false identification of a thawed state based on the SPL3FTP\_E product was detected for the area around the FB, SG and HV test sites (see Figure 3). As an example, Figure 3(a) shows the maps of FT state derived from SPL3FTP\_E product on January 1 each year from 2016 to 2019. The SPL3FTP\_E product determines the thawed state of landscape not only in the first days of

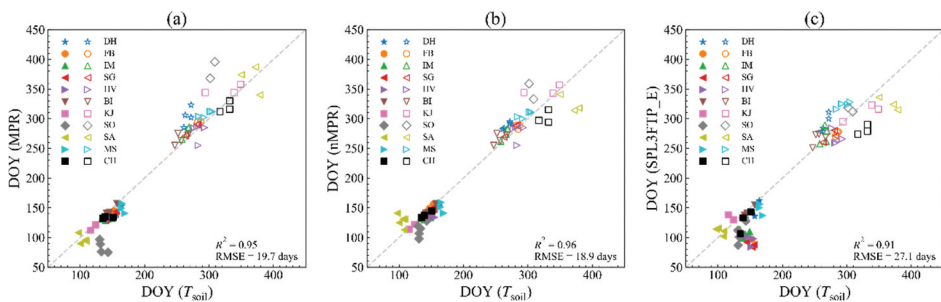


**Figure 2.** Dependence between day of year (DOY) of soil thaw (filled symbols)/freeze (open symbols) onsets based on MPR (a), nMPR (b) and SMAP SPL3FTP\_E product (c) and onsets based on a soil temperature from weather stations ( $T_{\text{soil}}$ ) during a period of 2015–2019. (Ascending orbits were used. The soil temperature above 0°C corresponds to values of MPR>1 and nMPR >0.75.).

**Table 2.** Accuracy in the determination of soil FT state for 12 test sites using the nMPR, MPR indices and data from the SPL3FTP\_E product, relative to the soil surface temperature.\*

Test site	ASC**			DESC**		
	nMPR	MPR	SMAP	nMPR	MPR	SMAP
DH	87/96/90	87/100/86	87/99/91	85/96/88	76/100/83	88/99/91
FB	97/94/96	97/100/94	67/96/76	86/97/88	85/100/88	63/99/72
SG	92/92/92	92/98/92	53/100/70	87/95/89	88/91/89	53/98/69
HV	91/80/87	91/80/87	56/93/70	91/91/91	93/47/76	56/88/68
IM	89/91/89	89/92/89	72/93/79	87/95/89	91/76/86	74/92/79
BI	94/99/96	94/98/96	95/90/97	93/99/94	93/95/94	94/99/95
BJ	86/65/65	86/65/65	100/90/59	75/65/65	88/55/56	88/55/56
KJ	86/91/89	86/96/89	90/90/86	82/97/90	88/88/88	92/78/84
SO	58/98/75	58/100/57	66/90/80	52/98/71	48/96/69	67/99/81
SA	91/77/81	91/92/84	85/90/80	84/81/82	71/90/84	90/76/80
MS	88/89/88	88/95/88	86/90/90	83/91/85	83/91/85	91/98/93
CH	96/85/89	96/93/91	90/90/84	94/88/91	93/89/91	92/79/85
<b>Number of observations</b>	7768/5498			7997/5266		
<b>Mean</b>	<b>88/91/86</b>	<b>81/95/85</b>	<b>79/97/77</b>	<b>83/95/85</b>	<b>83/83/82</b>	<b>79/95/79</b>
<b>Mean (Forest excluded)</b>	<b>92/91/91</b>	<b>88/95/90</b>	<b>76/95/82</b>	<b>88/94/89</b>	<b>88/86/87</b>	<b>76/94/82</b>

\* Days percentage to the total days number of satellites observation. The statistical data are separately given for the seasons with positive (red) and negative (blue) surface soil temperature. The statistical data for all seasons is given in black. \*\*ASC and DESC are the ascending and descending orbits, respectively.

January, but throughout January both in 2016 and in the next years 2017–2019 (see Figure 3(a)). However, data of FB, SG and HV weather stations show negative soil surface temperatures over this period. In addition, MODIS LST data (MYD11A1, averaged over 5 days) showed that thawed event (during January of each year from 2016 to 2019) was not caused by positive air temperature (see Figure 3(c)). MODIS LST more closely represents air temperature than soil surface temperature (Muzalevskiy and Ruzicka 2016)). Maps created using our own algorithm based on nMPR index also indicated this area as frozen (see Figure 3(b)).

## 5. Conclusion

The results of the validation carried out confirm the advantage of using the polarization index, calculated on the basis of estimates of the reflectivity of the soil, rather than directly using the brightness temperatures for determination FT state of soil surface. At the same time, the share of reliable cases of FT state determination increases by 3–9% in comparison with the standard SMAP product (SPL3FTP\_E). Further work is needed to validate the proposed approach using a broader set of test sites, including both Arctic and temperate regions, and also to compare between SMAP enhanced (9 km) and baseline (36 km) products due to their different noise levels. In view of the different observation angles of the brightness temperature by the satellites SMAP (40°) and GCOM-W1/AMSR2 (55°), it is necessary to investigate the advantages of the proposed method using SMOS (at fixed angle of 55°) instead of SMAP brightness temperature observations.

## Disclosure statement

No potential conflict of interest was reported by the authors.

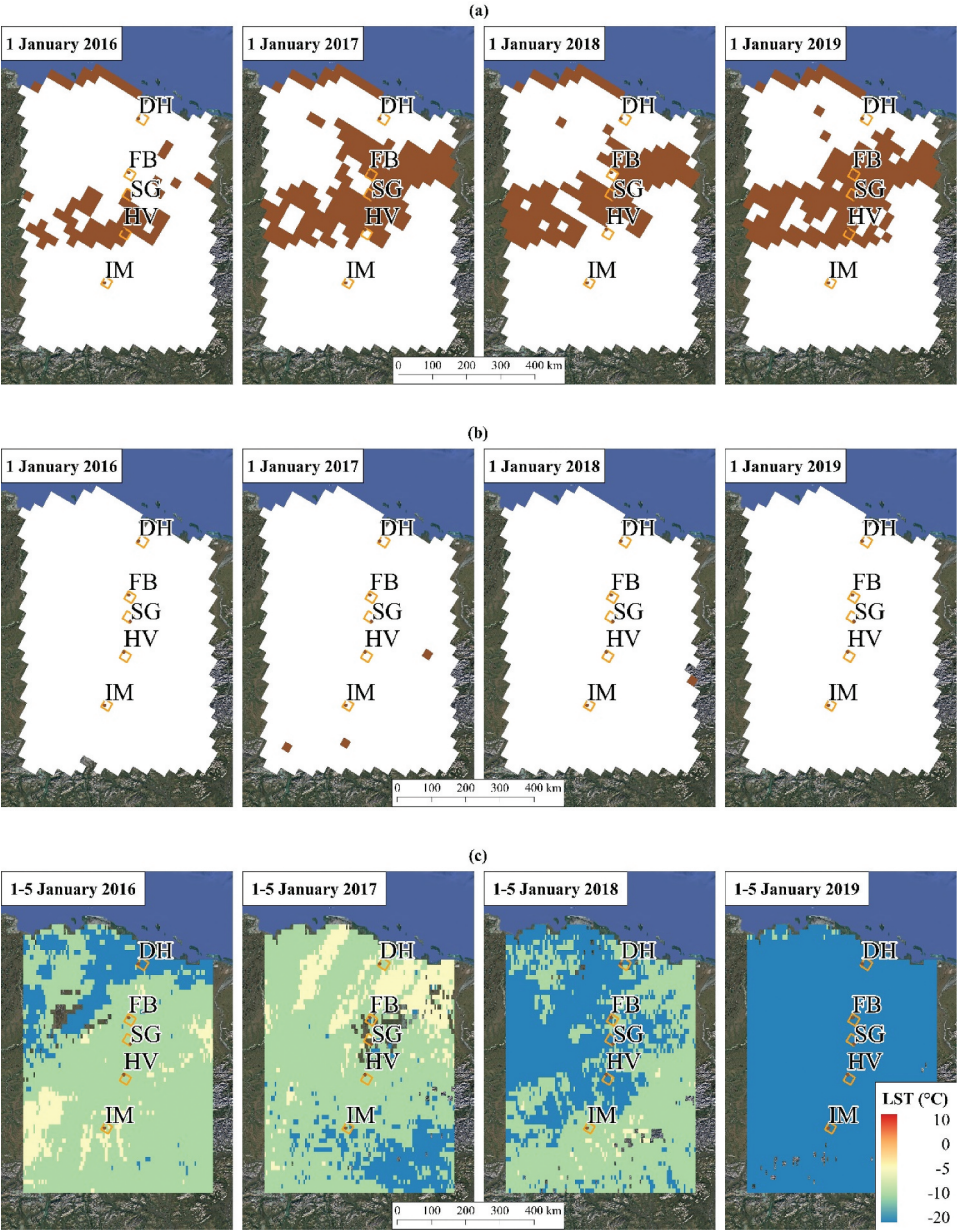


**Figure 3.** Maps of F/T state over latitudinal transect in North slope of Alaska for the period of 2016–2019 on January 1, derived from SMAP SPL3FTP\_E product (a), and our own algorithm nMPR index (b). White and brown colours correspond frozen and thawed state, respectively. Panel (c) depicts false colour images of LST (MODIS) in degrees Celsius.

## Funding

This work was supported by the SB RAS project No. 0287-2021-0034. Weather stations data was acquired and processing with support of Interdisciplinaire en Milieu Polaire), Université de Sherbrooke; GRIMP, NSERC and FRQNT; US National Science Foundation [PLR-1304464 and PLR-1417745]; 0287-2021-0034 [SB RAS]; State Research Programs [AAAA-A17-117051850059-6].

## References

- Derksen, C., X. Xu, R. S. Dunbar, A. Colliander, Y. Kim, J. S. Kimball, T. A. Black, et al. 2017. "Retrieving Landscape Freeze/Thaw State from Soil Moisture Active Passive (SMAP) Radar and Radiometer Measurements". *Remote Sensing of Environment* 194: 48–62. doi:10.1016/j.rse.2017.03.007.
- Dunbar, S., X. Xu, A. Colliander, C. Derksen, J. Kimball, and Y. Kim. 2016. "Algorithm Theoretical Basis Document (ATBD). SMAP Level 3 Radiometer Freeze/Thaw Data Products." *JPL CIT: JPL D-56288*: 33. ESA. 2017. "Land Cover CCI Product User Guide Version 2." *Technical Report*. [maps.elie.ucl.ac.be/CCI/viewer/download/ESACCI-LC-Ph2-PUGv2\\_2.0.pdf](https://maps.elie.ucl.ac.be/CCI/viewer/download/ESACCI-LC-Ph2-PUGv2_2.0.pdf)
- Fisher, R. A. 1936. "The Use of Multiple Measurements in Taxonomic Problems." *Annals of Eugenics* 7: 179–188. doi:10.1111/j.1469-1809.1936.tb02137.x.
- Hu, T., T. Zhao, J. Shi, S. Wu, D. Liu, H. Qin, and K. Zhao. 2017. "High-Resolution Mapping of Freeze/Thaw Status in China via Fusion of MODIS and AMSR2 Data." *Remote Sensing* 9: 1339. doi:10.3390/rs9121339.
- Hu, T., T. Zhao, K. Zhao, and J. Shi. 2019. "A Continuous Global Record of Near-surface Soil Freeze/thaw Status from AMSR-E and AMSR2 Data." *International Journal of Remote Sensing* 40 (18): 6993–7016. doi:10.1080/01431161.2019.1597307.
- Kilic, L., C. Prigent, F. Aires, J. Boutin, G. Heygster, R.T. Tonboe, H. Roquet, C. Jimenez, C. Donlon. 2018. "Expected Performances of the Copernicus Imaging Microwave Radiometer (CIMR) for an All-Weather and High Spatial Resolution Estimation of Ocean and Sea Ice Parameters." *J. Geophys. Res. Oceans* 123: 7564–7580.
- Muzalevskiy, K., and Z. Ruzicka. 2020. "Detection of Soil Freeze/Thaw States in the Arctic Region Based on Combined SMAP and AMSR-2 Radio Brightness Observations." *International Journal of Remote Sensing* 41 (14): 5046–5061. doi:10.1080/01431161.2020.1724348.
- Muzalevskiy, K. V., and Z. Ruzicka. 2016. "Retrieving Soil Temperature at a Test Site on the Yamal Peninsula Based on the SMOS Brightness Temperature Observations." *IEEE Journal of Selected Topics in Applied Earth Observations and Remote Sensing* 9 (6): 2468–2477. doi:10.1109/JSTARS.2016.2553220.
- Muzalevskiy, K. V., Z. Ruzicka, L. G. Kosolapova, and V. L. Mironov. 2016. "Temperature Dependence of SMOS/MIRAS, GCOM-W1/AMSR2 Brightness Temperature and ALOS/PALSAR Radar Backscattering at Arctic Test Sites." *Progress in Electromagnetic Research Symposium (PIERS), Shanghai*, 3578–3582.
- Rautiainen, K., J. Lemmetyinen, M. Schwank, A. Kontua, C. Ménarda, C. Mätzler, M. Drusch, A. Wiesmann, J. Ikonen, and J. Pulliainen. 2014. "Detection of Soil Freezing from L-band Passive Microwave Observations." *Remote Sensing of Environment* 147: 206–218. doi:10.1016/j.rse.2014.03.007.
- Rautiainen, K., T. Parkkinen, J. Lemmetyinen, M. Schwank, A. Wiesmann, J. Ikonen, C. Derksen, et al. 2016. "SMOS Prototype Algorithm for Detecting Autumn Soil Freezing." *Remote Sensing of Environment* 180: 346–360. doi:10.1016/j.rse.2016.01.012.
- Roy, A., A. Royer, C. Derksen, L. Brucker, A. Langlois, A. Mialon, and Y. H. Kerr. 2015. "Evaluation of Spaceborne L-band Radiometer Measurements for Terrestrial Freeze/thaw Retrievals in Canada." *IEEE Journal of Selected Topics in Applied Earth Observations and Remote Sensing* 8: 4442–4459.
- Walker, D., M. Reynolds, F. Daniëls, E. Einarsson, A. Elvebakk, W. A. Gould, A. E. Katenin, et al. 2005. "The Circumpolar Arctic Vegetation Map." *Journal of Vegetation Science* 16 (3): 267–282. doi:10.1111/j.1654-1103.2005.tb02365.x.

- Zhao, T., J. Shi, T. Hu, L. Zhao, D. Zou, T. Wang, D. Ji, R. Li, and P. Wang. 2017. "Estimation of High-resolution near Surface Freeze/thaw State by the Integration of Microwave and Thermal Infrared Remote Sensing Data on the Tibetan Plateau." *Earth and Space Science* 4: 472–484. doi:[10.1002/2017EA000277](https://doi.org/10.1002/2017EA000277).
- Zhao, T., L. Zhang, L. Jiang, S. Zhao, L. Chai, and R. Jin. 2011. "A New Soil Freeze/thaw Discriminant Algorithm Using AMSR-E Passive Microwave Imagery." *Hydrological Processes* 25 (11): 1704–1716. doi:[10.1002/hyp.7930](https://doi.org/10.1002/hyp.7930).